9-2013

Functional derivatives for uncertainty quantification and error estimation and reduction via optimal high-fidelity simulations

Alejandro Strachan
Birck Nanotechnology Center, Purdue University, strachan@purdue.edu

Sankaran Mahadevan
Vanderbilt University

Vadiraj Hombal
Vanderbilt University

Lin Sun
Birck Nanotechnology Center, Purdue University, sun33@purdue.edu

Strachan, Alejandro; Mahadevan, Sankaran; Hombal, Vadiraj; and Sun, Lin, "Functional derivatives for uncertainty quantification and error estimation and reduction via optimal high-fidelity simulations" (2013). *Birck and NCN Publications.* Paper 1462.
http://dx.doi.org/10.1088/0965-0393/21/6/065009

Functional derivatives for uncertainty quantification and error estimation and reduction via optimal high-fidelity simulations

2013 Modelling Simul. Mater. Sci. Eng. 21 065009

(http://iopscience.iop.org/0965-0393/21/6/065009)

Modelling Simul. Mater. Sci. Eng. **21** (2013) 065009 (20pp) doi:10.1088/0965-0393/21/6/065009

Functional derivatives for uncertainty quantification and error estimation and reduction via optimal high-fidelity simulations

Alejandro Strachan[1], **Sankaran Mahadevan**[2], **Vadiraj Hombal**[2] **and Lin Sun**[3]

[1] School of Materials Engineering and Birck Nanotechnology Center, Purdue University, West Lafayette, IN 47907, USA
[2] Department of Civil and Environmental Engineering, Vanderbilt University, Nashville, TN, USA
[3] School of Mechanical Engineering and Birck Nanotechnology Center, Purdue University, West Lafayette, IN 47907, USA

E-mail: strachan@purdue.edu

Received 10 January 2013, in final form 7 May 2013
Published 24 July 2013
Online at stacks.iop.org/MSMSE/21/065009

Abstract

One of the most fundamental challenges in predictive modeling and simulation involving materials is quantifying and minimizing the errors that originate from the use of approximate constitutive laws (with uncertain parameters and/or model form). We propose to use functional derivatives of the quantity of interest (QoI) with respect to the input constitutive laws to quantify how the QoI depends on the entire input functions as opposed to its parameters as is common practice. This *functional sensitivity* can be used to (i) quantify the prediction uncertainty originating from uncertainties in the input functions; (ii) compute a first-order correction to the QoI when a more accurate constitutive law becomes available, and (iii) rank possible high-fidelity simulations in terms of the expected reduction in the error of the predicted QoI. We demonstrate the proposed approach with two examples involving solid mechanics where linear elasticity is used as the low-fidelity constitutive law and a materials model including non-linearities is used as the high-fidelity law. These examples show that functional uncertainty quantification not only provides an exact correction to the coarse prediction if the high-fidelity model is completely known but also a high-accuracy estimate of the correction with only a few evaluations of the high-fidelity model. The proposed approach is generally applicable and we foresee it will be useful to determine where and when high-fidelity information is required in predictive simulations.

(Some figures may appear in colour only in the online journal)

1. Introduction

Current petascale computing resources and the planned exascale systems [1] provide an extremely powerful tool for predictive materials simulations [2–4]. The combination of such computing resources with advances in materials modeling at the electronic, atomic, meso- and macroscopic scales has the potential to significantly increase our understanding of materials behavior and revolutionize their design [5, 6], optimization and certification [7]. One of the main objectives of predictive materials modeling is to provide information that can be used for decision making; for example, assessing whether or not to experimentally pursue the fabrication and testing of a new material or device, or determining whether a material will perform to the desired level with a pre-determined level of confidence. For simulations to play a central role in such a decision-making process, the confidence in the predicted results should be quantified. This process is known as validation and can only be carried out against appropriate experiments and after the various errors and uncertainties involved in the simulations and experiments are quantified. Thus, significant efforts have been devoted to the quantification of the various types of errors and uncertainties that arise in modeling, see, for example, [8–14] and in experiments, see, for example, [15].

Experimental validation can be complemented by quantifying the uncertainty of a prediction with respect to a higher-fidelity model. This is becoming increasingly important with the wide hierarchy of atomistic methods (from quantum Monte Carlo to large-scale molecular dynamics) capable of providing fundamental information to predict materials behavior with high accuracy. Furthermore, multiscale modeling approaches involving various combinations of atomistic, mesoscale and macroscale simulations are currently being pursued for essentially every class of materials type and for a variety of devices. The quantification of errors introduced in the process of upscaling is critical before these methods can be incorporated into design and certification cycles. Thus, given the increasing computing power available and the advances in materials modeling at all scales, uncertainty and error quantification of a predicted quantity of interest (QoI) in terms of high-fidelity, finer-scale simulations is becoming a key challenge in predictive modeling and high-performance computing.

Physics-based models of devices, components or products use constitutive laws to describe the response of the materials involved; these functions are typically obtained empirically prior to the simulation and are known only approximately. Examples include stress–strain relationships in solid mechanics, temperature- and pressure-dependent viscosity in fluid simulations and interatomic potentials for atomistic simulations. Even electronic structure density functional theory calculations are based on approximate exchange and correlation functionals. In general, these functions are not known exactly and their use leads to errors in the predictions. The uncertainty in constitutive laws includes that in its parameters but also the functional forms itself; this last uncertainty is often referred to as model form. Fortunately, higher-fidelity simulations are often available to refine these constitutive laws. However, such high-fidelity simulations are often computationally intensive and cannot be performed everywhere they are needed to replace the use of a constitutive law. For example, molecular dynamics simulations involving billions of atoms or large-scale dislocation dynamics simulations may be desirable to inform structural simulations of polycrystalline metals. Given the computational intensity of these simulations, one would like to identify the conditions for which the constitutive laws need to be improved most critically in order to obtain the highest error reduction given a computational budget and know how to use this information optimally.

This paper deals with the common case where a simulation code uses a computationally efficient but approximate constitutive law (input function) to predict a single QoI; we assume

that this *low-fidelity* constitutive law can be improved for specific values of its independent variable via high-fidelity, computationally-intensive simulations. The challenges addressed here are (i) quantifying the uncertainty in the predicted QoI originating from uncertainties in the low-fidelity input function; (ii) estimating a correction to the predicted QoI if a more accurate constitutive law becomes available and (iii) ranking possible high-fidelity simulations in terms of the expected reduction in the error in the QoI to produce a result with minimized uncertainties given a computational budget. We show that the functional derivatives of the QoI with respect to the input constitutive laws provide the key information needed to address these challenges.

The rest of the paper is organized as follows. Section 2 describes the proposed approach based on functional derivative to uncertainty quantification and error estimation. Section 3 describes the development of a Gaussian process surrogate model to compute the functional discrepancy in a sequential manner utilizing a few, but optimally designed, evaluations of the high-fidelity model. Sections 4 and 5 exemplify the use of our approach via two solid mechanics problems. Conclusions are drawn in section 6.

2. Functional derivatives for uncertainty quantification and minimization

When a computational model is used to predict a material property or process, the QoI can be thought of as a functional of the constitutive laws being used. In a general case, the QoI (Q) depends on a set of input parameters $\{P_i\}$ (e.g. geometry, environmental conditions, etc) and a set of constitutive functions f_i (e.g. stress–strain relationship):

$$Q = Q\left(\{P_i\}, \{f_i(z_i; Q_i)\}\right), \tag{1}$$

where z_i are the independent variables of function f_i which also depends on a set of parameters Q_i.

Typically, uncertainty quantification efforts include the characterization of the dependence of the QoI with respect to the various input parameters in the model $\{P_i\}$ and $\{Q_i\}$. This approach provides valuable information but has two significant shortcomings: (i) it assumes the functional forms of the constitutive laws to be correct and (ii) does not provide information regarding the region in the constitutive law (range of its independent variables) that dominates the QoI. To address these issues we propose to use the functional derivative of the QoI with respect to the constitutive law.

To simplify the nomenclature we will formulate functional uncertainty quantification in terms of a QoI that depends on a single constitutive law: $Q[f]$. Cases with multiple constitutive laws can be described in a similar way and constitutive laws with multiple independent variables will be demonstrated in section 5. The QoI is a functional that maps the space of functions (that satisfy certain properties) into the real domain: $Q : M \to \mathbb{R}$. We will use a definition of functional (Fréchet) derivative, $\frac{\delta Q[f]}{\delta f(z)}$, in terms of the functional differential [16]:

$$\delta Q[f] = \int \frac{\delta Q[f]}{\delta f(z)} \delta f(z)\, \mathrm{d}z, \tag{2}$$

where δf is any variation of f. This functional derivative is a distribution that quantifies how the model prediction depends on the entire constitutive law under use as opposed to its parameters. It can be thought of as an extension of the differential of a multivariate function ($\mathrm{d}Q = \sum_i \partial Q/\partial f_i \, \mathrm{d}f_i$) to infinite dimensions. The functional derivative depends on z and quantifies the sensitivity of the QoI with respect to the input function f at each value of z. This dependence on z and the meaning of functional derivative are perhaps more apparent when

Dirac's delta is used as the functional variation; this provides a definition of the functional derivative in terms of a quotient [16]:

$$\frac{\delta Q[f]}{\delta f(z)}(z_0) = \lim_{\epsilon \to 0} \frac{Q[f(z) + \epsilon \delta(z - z_0)] - Q[f(z)]}{\epsilon}. \tag{3}$$

The functional derivative of the QoI with respect to the input constitutive laws will be denoted *functional sensitivity* and the following sub-section will focus on its use to (i) estimate the uncertainty in the prediction given uncertainties in the constitutive law, (ii) correct the predicted QoI if a more accurate constitutive law becomes available and (iii) rank possible high-fidelity simulations to locally refine the constitutive law according to their expected error reduction in the QoI.

2.1. Uncertainty quantification

An important component of uncertainty quantification efforts is the propagation of uncertainties in the input parameters through the model to quantify how they affect the prediction. In our case we are interested in propagating uncertainties in the input function itself as opposed to its parameters. Equation (2) can be used to obtain, to first order in f, a bound in the uncertainty in the QoI if the absolute deviation of the low-fidelity constitutive law as a function of z can be quantified:

$$\Delta Q_{UQ} = \int \left| \frac{\delta Q[f]}{\delta f(z)} \right| \Delta f(z)\, \mathrm{d}z, \tag{4}$$

where Δ_f denotes the absolute uncertainty in $f(z)$. In cases where the error in the constitutive law can be bound or the QoI is not a linear functional of the constitutive law, equation (4) provides a very useful estimate of the uncertainty in the calculation. Note that the expression in equation (4) leads to a non-negative number and is a generalization of the standard expression of multivariate absolute error propagation to the continuum.

2.2. Error reduction

The definition of the functional derivative, equation (2), also provides a prescription to correct the predicted QoI if a more accurate constitutive law becomes available either via additional experiments or high-fidelity simulations. Let $g(z)$ denote the high-fidelity constitutive law, a corrected prediction is obtained by replacing the variation of f with $(g(z) - f(z))$:

$$\Delta Q_{\mathrm{corr}} = \int \frac{\delta Q[f]}{\delta f(z)} \left(g(z) - f(z)\right)\, \mathrm{d}z. \tag{5}$$

This expression represents an integral of the functional sensitivity multiplied by the functional discrepancy and is an extension of the widely used expression for discrete input variables to functions. Note that, in contrast to the non-negative uncertainty, this correction can be negative or positive.

2.3. Ranking of high-fidelity model evaluation for error reduction

As discussed above, in continuum simulations of devices or components involving materials simulations (as well as in many other fields) it is possible to refine the constitutive laws used to predict the QoI via finer grain simulations. However, these high-fidelity simulations can be computationally intensive (e.g. dislocation dynamics of *ab initio* calculations) and often cannot be carried out for all possible (or likely) values of the independent variable z. Thus, one would like to know the values of z where these physics-enhancement simulations would

have the highest impact in reducing the error of the predicted QoI. The functional derivative expression in equation (5) provides the answer. The integrand in equation (5), i.e. product of the functional sensitivity times the functional discrepancy, $\frac{\delta QoI}{\delta f(z)}(g(z) - f(z))$, provides a measure of the error in the QoI introduced by the constitutive model as a function of the independent variable z and, consequently, ranks in importance the high-fidelity simulations that need to be performed.

While formally equation (5) is very valuable, from a practical point of view its use is not straightforward since the quantity $\frac{\delta QoI}{\delta f(z)}(g(z) - f(z))$ depends on the enhanced constitutive law $g(z)$, which we are trying to evaluate only when needed and for a relative small number of cases. In section 3 we discuss how discrepancy modeling together with functional UQ can be used to *orchestrate* high-fidelity simulations using Gaussian processes within a Bayesian approach to build increasingly accurate approximations to the functional discrepancy $(g(z) - f(z))$ in a sequential manner using a few evaluations of the high-fidelity model.

In sections 4 and 5 and we provide examples of the use of equation (5) to correct the prediction using a more accurate constitutive law. We first assume the high-fidelity function is known to exemplify the approach and then show how the functional discrepancy can be approximated in a sequential manner requiring a few evaluations of the high-fidelity model.

3. Discrepancy modeling for physics enhancement selection

As discussed above, evaluation of the functional error in the QoI involves the functional sensitivity $S(z) = \frac{\delta QoI}{\delta f(z)}$ and the discrepancy $E(z) = g(z) - f(z)$ for all values of the independent variable z that are relevant for the calculation of the QoI. Since the sensitivity depends only on the low-fidelity model, $f(z)$, it may be evaluated efficiently during the device simulation. On the other hand, evaluation of the discrepancy $E(z)$ everywhere is computationally unaffordable since it depends on the high-fidelity model $g(z)$. To alleviate this problem, we propose the estimation of the error in the QoI using a computational surrogate to $E(z)$ that is inexpensive to evaluate. Such an approximation is developed using data collected from evaluations of the high-fidelity model at a small subset of values (z_i) of the independent variable z. Note that the discrepancy $E(z)$ may be estimated either by replacing the high-fidelity simulation $g(z)$ with a data-based approximation $\bar{g}(z)$ or by replacing the discrepancy $g(z) - f(z)$, with a data-based approximation $\bar{E}(z)$; since the low-fidelity law $f(z)$ would capture some of the physics of the problem we expect the discrepancy to be easier to describe with a surrogate model than the physics-enhancement law itself. In either case, the corresponding approximation is developed based on the evaluation of the high-fidelity model at carefully selected data points. The appendix provides background information and additional information about surrogate models.

The accuracy of the approximation depends on the basis functions used to develop the approximation and on the selection of the data points z_i, at which the high-fidelity model is evaluated. The two factors are interlinked—the utility of the data depends on the ability of the basis functions to extract information from the data. On the other hand, accurate approximation for a given set of basis functions depends on the amount and quality of data.

3.1. Models for discrepancy

The bases employed for approximation may be broadly classified as either local or global. Global bases are active throughout the domain and are therefore efficient in modeling trends. They require uniformity in the spread of the data throughout the domain. Local bases are parametrized by basis location and size, and are only active within a neighborhood of their

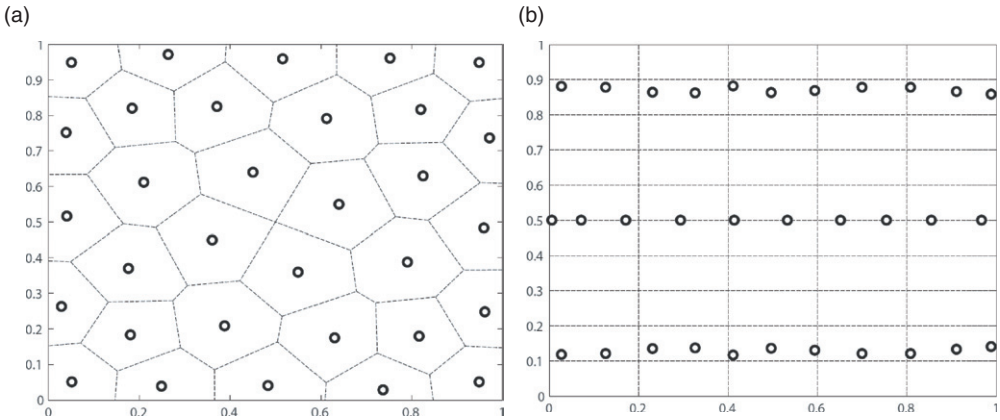

Figure 1. Data point designs for functions with uniform variation throughout the domain. Optimal designs from variance minimizing data point selection for (*a*) functions with same level of variation in both the dimensions (isotropic), and (*b*), with different levels of variation in the two dimensions (anisotropic).

location. They are therefore efficient in modeling localized variations in the domain and also allow for the data points to be localized. From the perspective of the problem at hand, the selection of appropriate bases for the approximation of discrepancy depends on its functional behavior in the domain. If the discrepancy is smooth with uniform variation throughout the domain, then it can be modeled efficiently using global bases. On the other hand, if discrepancy has localized variations, then global basis functions cannot be efficiently employed, and local or quasi-local bases are required to achieve efficiency.

We propose to model the discrepancy as a particular realization of a Gaussian process defined over the domain of z. The Gaussian process is completely characterized by its mean and covariance functions, both of which may be constructed using parametrized global and local functions [17]. This allows us to systematically develop an approximation to model discrepancy using both global and local bases depending on the nature of discrepancy.

3.2. Data point selection

Since $g(z)$ is expensive to evaluate, its properties, such as its functional variation, cannot be determined *a priori*. The construction of the approximate model is therefore sequential and employs an iterative procedure involving adaptive selection of training points and estimation of the approximate model. The parameters of the Gaussian process provide information on the variation of the model discrepancy, and can be used to guide the adaptive selection of training points. However, the procedure could be affected by the choice of initial training points or covariance functions, and needs to be implemented with caution.

When the model discrepancy is even and spread throughout the domain, a design of the data points that are spread uniformly over the domain is necessary and efficient. Such designs may be obtained through a variance minimizing data point selection algorithm which selects the data points so as to minimize the total prediction variance over the entire domain. As seen in figure 1, the key to the design of data points here is consistency of variation throughout the domain, even if it is different for each dimension of the domain.

However, if the variation in model discrepancy is localized to only a small part of the domain, and is smooth otherwise, uniform sample distributions based on local variations represent an inefficient use of the scarce data resources (see figure 2). In such cases the

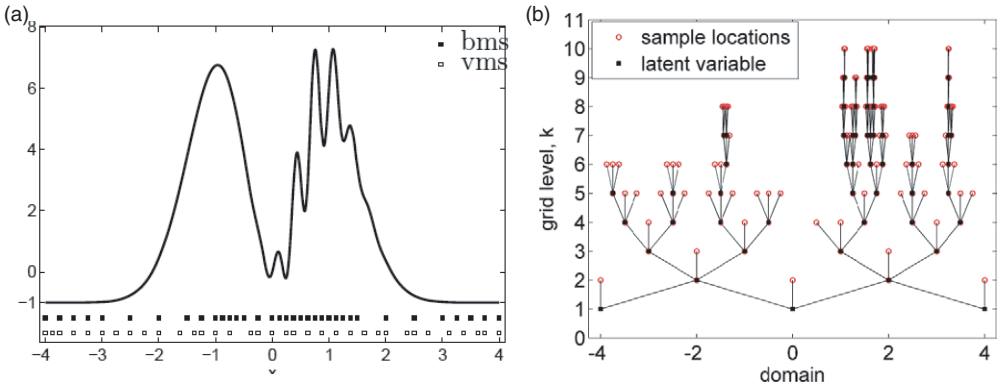

Figure 2. An example of localized discrepancy with localized variation (thick line in panel A). The corresponding variation sensitive hierarchical model (*b*), and the variation sensitive data designs (dots at the bottom of (*a*)).

localized bases of the Gaussian processes may be leveraged to develop a sequential model that hierarchically achieves coarse-to-fine decomposition of the discrepancy. Since the size and the location of the bases depend on the size and location of the local variation, this method provides a localization for the *a priori* unknown features of the model discrepancy. Such a decomposition therefore yields insights into the nature of deficiency of the constitutive model (see figure 2). In addition since each layer of the model approximates the error in approximation due to the previous layers, the resulting model provides a bias minimizing reconstruction of the model discrepancy. Refer to [18] for details of the bias minimizing selection of sampling locations using the concept of sparse Gaussian processes.

In terms of computational effort in evaluating $g(z)$, since localized bases only require data within the support of the bases, a hierarchical decomposition provides a variation sensitive data design in which the data density corresponds to the variation in the model discrepancy—with high data density only in the regions where the discrepancy has a large variation.

The key to the development of such a model is the identification of the location of the centers of the bases and their size. While the use of a geometric structure such as a tree allows for efficient localization of the bases, the size of the bases depends on the underlying variation. Since Gaussian process regression is a probabilistic regression technique, it allows for systematic integration of prior information about the variation in the model discrepancy. In addition, the entire predictive distribution at each layer can be incorporated within a robust Bayesian inference framework that allows for the quantification of uncertainty due to sparseness of data and provides a probabilistic data point selection criteria that allows for a balance between bias and variance in the estimation of the model discrepancy.

In summary, the choice of basis function for the development of approximation depends on the behavior of the model discrepancy. If the model discrepancy is found to be smooth in some region, the training data locations are selected based on variance minimization, and if the model discrepancy contains localized variations, the training data locations are selected based on bias minimization. Such an adaptive procedure can achieve both computational efficiency and accuracy.

3.3. Importance of the functional sensitivity of QoI

By considering the quality of the approximation over the entire domain, the constructed approximation exhibits high fidelity to the actual model discrepancy and thus provides accurate

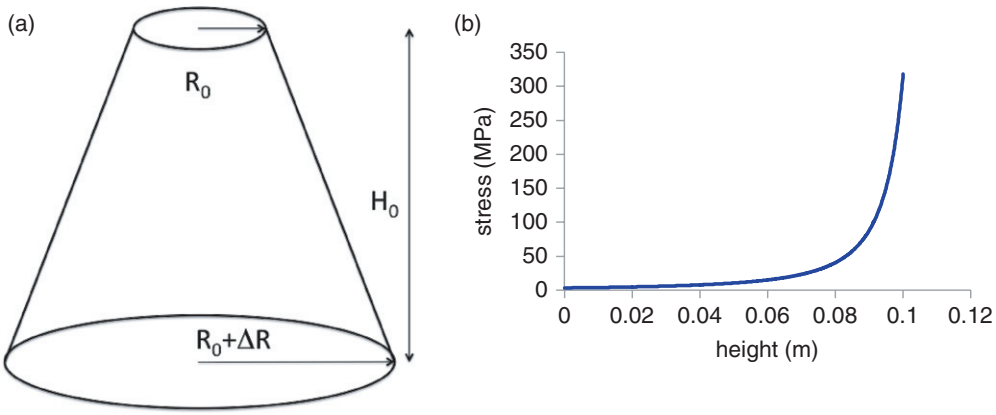

Figure 3. (*a*) Geometry of the truncated cone whose deformation is to be predicted. (*b*) Stress as a function of height in the undeformed cone for an applied force of 100 kN.

estimation of it throughout the domain of the independent variable z. However, in the estimation of the QoI functional error, model discrepancy is weighted by the sensitivity, $S(z)$. For values of z for which the sensitivity is infinitesimally small, the contribution of the model discrepancy to the computation of QoI is nullified. Evaluation of the computationally expensive high-fidelity model $g(z)$ in these regions is therefore wasteful. Instead, the sensitivity $S(z)$ may be employed to identify regions of interest within the overall domain of z, and the sampling algorithm may then be employed only within this region. One possible approach is to consider the convex hull of the regions obtained by the thresholding of the input distribution as the domain of interest. Another possible approach is to weight the residue at a potential sampling point with the sensitivity of QoI. For unimodal sensitivity distributions, with large variances, the two approaches are likely to provide similar samples. However, for input distributions with concentrated sensitivity distributions but with long tails, the thresholding approach is preferable, since the weighting approach is likely to concentrate the sampling according to the sensitivity distribution rather than the variation in the model discrepancy.

4. Example 1: compression of a conical specimen

In this section we exemplify the proposed approach with a simple, computationally trivial, problem. We are interested in predicting the deformation of a truncated cone, see figure 3(*a*), with initial height $H_0 = 10\,\text{cm}$, top radius $R_0 = 1\,\text{cm}$ and base radius $R_0 + \Delta R = 10\,\text{cm}$, when a compressive force $F = 100\,\text{kN}$ is applied to it. To keep the calculations simple and to focus on the proposed approach we will neglect the height-dependent lateral expansion due to Poisson's effect and treat the system as one dimensional. Under these conditions the problem becomes one dimensional and subscripts indicating directions will be ignored in stress and strain; σ and ϵ denote for the rest of the section diagonal components of the stress and strain tensors in the vertical (r_3) direction. The stress is a function of position:

$$\sigma(r_3) = \frac{F}{A(r_3)}, \tag{6}$$

where $A(r_3)$ is height-dependent area:

$$A(r_3) = \pi \left(R_0 + \frac{H_0 - r_3}{H_0} \Delta R \right)^2. \tag{7}$$

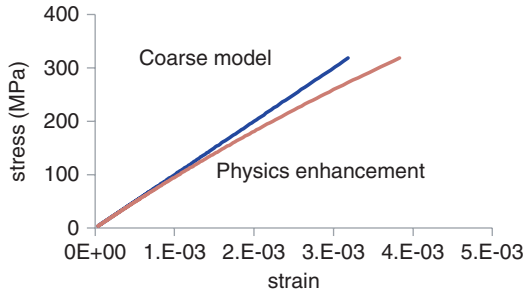

Figure 4. Constitutive laws used for coarse grain model (linear elasticity) and physics enhancement (non-linear stress–strain).

Figure 3(*b*) shows the engineering stress as a function of position in the undeformed cone for an applied force of 100 kN, remember that in this simple example we are ignoring transverse relaxation so engineering and true stress are equal.

The deformation of the specimen can then be computed using a material-specific constitutive equation that relates strain along r_3 and σ $[\epsilon(\sigma)]$ using the following expression:

$$H = \int_0^{H_0} (1 + \epsilon(r_3))\ \mathrm{d}r_3 = H_0 + \int_0^{H_0} \epsilon(r_3)\,\mathrm{d}r_3 \tag{8}$$

We will use a linear elastic model as the low-fidelity constitutive law for our material: $f(x) \rightarrow \sigma_{\mathrm{LF}}(\epsilon) = E\epsilon$; the subscript LF denotes low-fidelity. We assume that the material exhibits non-linear elasticity and is accurately described by the high-fidelity law: $f(x) \rightarrow \sigma_{\mathrm{HF}}(\epsilon) = E^*(1 - \exp(-\beta\epsilon))$; HF indicates high fidelity. Young's modulus of the material is 100 GPa and its non-linear constitutive law is described by $E^* = 1$ GPa and β=100, see figure 4.

Using finite differences, the total height reduction of the cone due to the 100 kN force is calculated to be 3.1863×10^{-5} m using the low-fidelity model and slightly higher, 3.4033×10^{-5} m, using the high-fidelity model. These numbers are obtained using 5000 points to integrate equation (8) with finite differences; the value for the low-fidelity model is very close to the exact analytical value of 3.1831×10^{-5}. The difference between the predictions of the two models originates for the softening of the non-linear constitutive law for large strains. In what follows we estimate the error in the prediction of H from the low-fidelity constitutive law using functional derivatives.

In order to compute the functional derivative in equation (2) we re-write equation (8) as an explicit functional of the strain-stress function:

$$H[\epsilon(\sigma)] = H_0 + \int_{\sigma(r_3=0)}^{\sigma(r_3=H_0)} \epsilon(\sigma)\frac{\mathrm{d}r_3}{\mathrm{d}\sigma}\,\mathrm{d}\sigma. \tag{9}$$

The functional derivative of the QoI (H) with respect to the constitutive law ($\epsilon(\sigma) = E/\sigma$) can be obtained from equation (9) by inspection using the definition in equation (2):

$$\frac{\delta H[\epsilon(\sigma)]}{\delta\epsilon(\sigma)} = \frac{\mathrm{d}r_3}{\mathrm{d}\sigma}. \tag{10}$$

Equation (10) describes how the height of the deformed cone depends on the strain at each value of stress experienced by the cone according to the low-fidelity constitutive law $[\sigma(r_3 = 0) : \sigma(r_3 = H_0)]$; the r_3 dependence of this function is shown in figure 5(*a*). This functional derivative shows that the strain for small stresses dominates the QoI prediction.

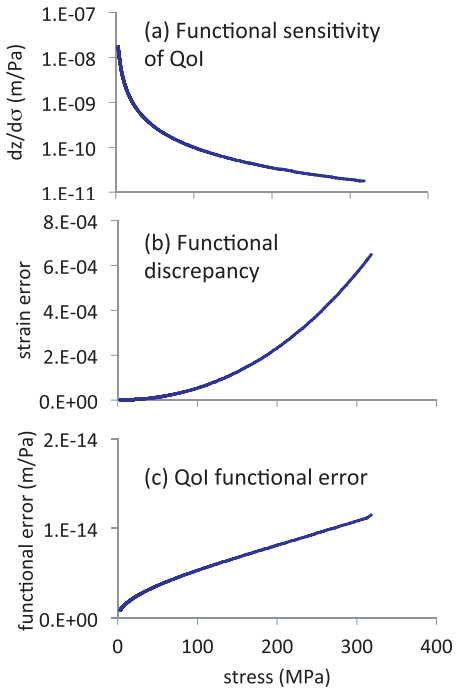

Figure 5. (*a*) Functional derivative of cone height with respect to input constitutive law, $\epsilon(\sigma)$, using coarse grain model. (*b*) Model error in strain $g(z) - f(z)$ as a function of stress. (*c*) Product of functions (*a*) and (*b*) gives *QoI functional error* to first order.

This, perhaps surprising, result is due to the non-linear distribution of stress along r_3: a larger fraction of the cone's height experiences low strains and stresses, see figure 3. Figure 5(*b*) shows functional discrepancy, i.e. the error in strain of the coarse constitutive law as compared with the physics-enhancement law ($g(z) - f(z)$). As described above, the product of these two functions provides a first-order estimate of the error in the QoI originating from the strain at each stress value; this *QoI functional error* provides a correction to the model prediction using the low-fidelity constitutive law when a higher accuracy, physics-enhanced, law becomes available.

A first-order correction to the low-fidelity prediction can be obtained by integrating the QoI functional error, equation (5), for all values of the independent variable. In the case of the deformed cone the correction takes the form

$$\Delta H = \int_{\sigma(r_3=0)}^{\sigma(r_3=H_0)} \frac{\mathrm{d}r_3}{\mathrm{d}\sigma} \left(\epsilon_{\mathrm{HF}}(\sigma) - \epsilon_{\mathrm{LF}}(\sigma)\right) \mathrm{d}\sigma. \tag{11}$$

The correction estimate from equation (11) is $2.170\,932 \times 10^{-6}$ m; this value is also obtained using finite differences. Adding this correction to the low-fidelity model result (3.1863×10^{-5} m) leads, exactly, to the result obtained numerically with the high-fidelity constitutive. The fact that the first-order correction leads to an exact result is due to the fact that the QoI is a linear functional of the constitutive law, see equation (9). It is important to highlight that this is true even if the functionals themselves are non-linear; the correction is exact if the QoI is a linear functional of the constitutive law. While the example is simple, obtaining an exact result without having to perform a new simulation with the high-fidelity model even when the form of the constitutive law changes is non-trivial.

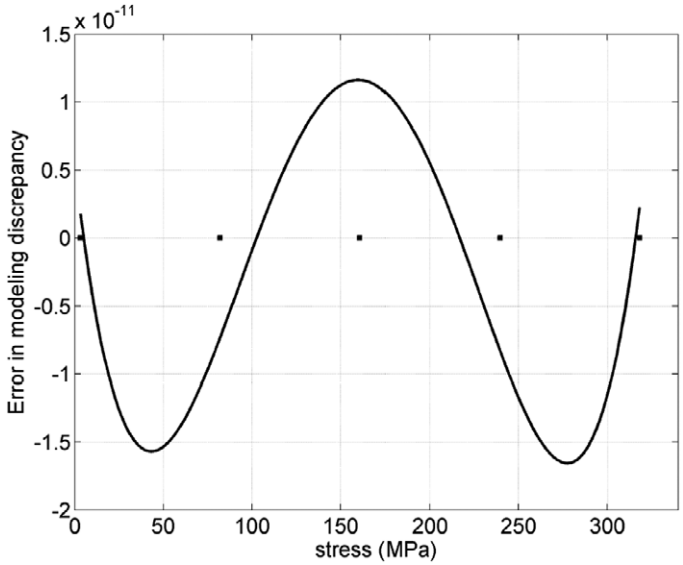

Figure 6. Error in modeling the discrepancy.

4.1. Design of optimal physics-enhancement simulations for uncertainty quantification and prediction correction

We showed that if the physics-enhancement law $g(z)$ is completely known our functional derivatives approach provides an exact correction to the CG prediction. However, in many cases of practical interest the physics-enhancement law is unknown but a simulation can be performed to evaluate it for specific values of its independent variable z. In this sub-section we discuss how the discrepancy function $(g(z) - f(z)$ can be sequentially built via optimally designed evaluations of the high-fidelity model. In the example at hand, see figure 5, since the functional sensitivity is of the order $O(10^{-3})$ and the functional discrepancy is of the order $O(10^{-5})$ their product is approximately constant throughout the domain. Hence the entire domain is relevant to the computation of the enhancement law and is selected by both the threshold or weighted threshold methods. Each high-fidelity simulation shows that the discrepancy in the model varies smoothly throughout the domain, and is therefore appropriately modeled by a Gaussian process model with a squared exponential covariance function (see section 3); and the variance minimizing approach is effective in identifying the best values of z at which to evaluate the high-fidelity model.

As seen in figure 6, only five evaluations of the high-fidelity model are needed to reduce the discrepancy between the actual high-fidelity model and its Gaussian process approximation to the order $O(10^{-11})$. Using the surrogate model for the discrepancy the first-order correction to the QoI is estimated to be 2.1896×10^{-6}, which is very close to the exact correction $(2.197\,092 \times 10^{-6})$.

Figure 6 shows the discrepancy between the actual high-fidelity model and its Gaussian process approximation. The values of z at which the high-fidelity model is evaluated are shown as solid dots in the figure. As seen in figure 6, only five evaluations of the high-fidelity model are needed to reduce the discrepancy between the actual high-fidelity model and its Gaussian process approximation to the order $O(10^{-11})$. Using the surrogate model for discrepancy, the first-order correction to the QoI is estimated to be 2.1896×10^{-6}, which is very close to the exact correction $(2.170\,932 \times 10^{-6})$.

5. Example 2: elastic force in a RF-MEMS switch cantilever

5.1. Problem description and simulation details

In this section we apply the functional sensitivity approach to a second, computationally more challenging, problem. We are interested in predicting the total elastic restoring force experienced by the cantilever of a radio frequency (RF) micro-switch [19]. The switch consists of a metallic cantilever fixed on one end and free on the other that lies over a dielectric landing pad below which is a signal line. In its relaxed configuration a 3 μm air gap separates the cantilever and the dielectric; under such conditions the switch exhibits a very low capacitance and an RF signal can go through it. The device is operated electrostatically by applying a voltage between the signal line (or a nearby actuation electrode) and the metallic beam; the electrostatic force causes the beam to deflect and eventually close, making contact to the dielectric pad. The capacitance of this state is very large and the RF signal is diverted into the beam.

The QoI we will focus on is the total restoring elastic force in the vertical (r_3) direction acting on the beam when it is in contact with the dielectric actuated by 100 V. The dimensions of the cantilever are 250 μm in length (along r_1), 120 μm in width (along r_2) and 1.5 μm in thickness. We use the MEMOSA simulation code [20] to predict the profile of the cantilever under the desired applied voltage using finite volumes. Due to the high aspect ratio of the micro-cantilever the Mindlin–Reissner plate theory is used to compute the beam deflection under electrostatic load [20]. A regular 2D quad mesh with 100×48 cells is used in simulation. The simulation provides the strain and stress tensor of the beam when it is at equilibrium contact position.

The low-fidelity model used in the beam simulation is, as in the example above, a linear elastic, isotropic constitutive law for the beam where the stress components are given in terms of the strain as

$$\sigma_{11} = E\,(\epsilon_{11} + \nu\epsilon_{22}) \tag{12}$$

$$\sigma_{22} = E\,(\epsilon_{22} + \nu\epsilon_{11})\,, \tag{13}$$

where $E = 200$ GPa is Young's modules and ν =0.3 is Poisson's ratio.

The high-fidelity model is taken as a non-linear elastic law equivalent to that in section 4:

$$\sigma_{11} = \begin{cases} E^*\left[1 - \exp\left(-\beta\,|\epsilon_{11} + \nu\epsilon_{22}|\right)\right] & \text{if } (\epsilon_{11} + \nu\epsilon_{22}) > 0 \\ -E^*\left[1 - \exp\left(-\beta\,|\epsilon_{11} + \nu\epsilon_{22}|\right)\right] & \text{otherwise} \end{cases} \tag{14}$$

$$\sigma_{22} = \begin{cases} E^*\left[1 - \exp\left(-\beta\,|\epsilon_{22} + \nu\epsilon_{11}|\right)\right] & \text{if } (\epsilon_{22} + \nu\epsilon_{11}) > 0 \\ -E^*\left[1 - \exp\left(-\beta\,|\epsilon_{22} + \nu\epsilon_{11}|\right)\right] & \text{otherwise,} \end{cases} \tag{15}$$

where $E^* = 2$ GPa and β =100 are chosen to lead to the same initial slope as the low-fidelity model and to non-linear elasticity.

5.2. QoI and functional sensitivity

The total elastic force in the vertical (r_3) direction of the switch is obtained within the plate approximation used in the simulations as an integral over the cantilever area (A_0):

$$F = \int_{A_0} h_0 \left[\frac{\partial \sigma_{11}(r_1, r_2)}{\partial r_1} \frac{\partial w(r_1, r_2)}{\partial r_1} + \frac{\partial \sigma_{22}(r_1, r_2)}{\partial r_2} \frac{\partial w(r_1, r_2)}{\partial r_2} \right] \mathrm{d}r_1\,\mathrm{d}r_2. \tag{16}$$

where $w(r_1, r_2)$ is the beam height as a function of position. In this equation, the stress derivatives give forces along the plane of the beam and the derivatives of the beam height with

respect to r_1 and r_2 project these forces along the r_3 direction. We note that, when integrated, the term involving σ_{22} yields zero due to symmetry. The remaining term can be modified to provide an expression for the functional derivative of the QoI with respect to the constitutive law (stress as a function of strain). We first use integration by parts to obtain

$$F = h_0 \int \left[\sigma_{11}(r_1, r_2) \frac{\partial w(r_1, r_2)}{\partial r_1} \right]\Bigg|_{x_0}^{x_1} \mathrm{d}r_2 - h_0 \int_{A_0} \sigma_{11}(r_1, r_2) \frac{\partial^2 w(r_1, r_2)}{\partial r_1^2} \, \mathrm{d}r_1 \, \mathrm{d}r_2, \tag{17}$$

where the first term is evaluated at the cantilever boundaries along the r_1 direction leading to zero. The second term can be re-arranged in terms of an integral over strain values to provide an expression for the functional derivative:

$$\begin{aligned} F &= h_0 \int_{A_0} \sigma_{11} \left(\epsilon_{11}(r_1, r_2), \epsilon_{22}(r_1, r_2) \right) \frac{\partial^2 w(r_1, r_2)}{\partial x^2} \, \mathrm{d}r_1 \, \mathrm{d}r_2 \\ &= \int \sigma_{11}(\epsilon_{11}, \epsilon_{22}) \frac{\delta F}{\delta \sigma_{11}}(\epsilon_{11}, \epsilon_{22}) \, \mathrm{d}\epsilon_{11} \, \mathrm{d}\epsilon_{22}. \end{aligned} \tag{18}$$

From equation (18) we can write the functional derivative of the vertical force with respect to the input stress–strain function as

$$\frac{\delta F}{\delta \sigma_{11}}(e_{11}, e_{22}) = h_0 \int_{A_0} \delta(e_{11} - \epsilon_{11}(r_1, r_2), e_{22} - \epsilon_{22}(r_1, r_2)) \frac{\partial^2 w(r_1, r_2)}{\partial x^2} \, \mathrm{d}r_1 \, \mathrm{d}r_2. \tag{19}$$

We compute the functional derivative $\frac{\delta F}{\delta \sigma_{11}}(e_{11}, e_{22})$ from equation (19) numerically based on the low-fidelity solution discretizing strain ϵ_{11} between -0.002 and $+0.003$ and ϵ_{22} between -0.0008 and $+0.0028$ with a 50×50 grid.

5.3. Results

Figure 7 shows the membrane height (*a*), the diagonal component of the strain in the r_1 direction (ϵ_{11}) (*b*), and the contribution to the force along r_3 of each cell from equation (18) (*c*) as a function of position along the beam's length. In figure 7(*c*) squares represent the low-fidelity model and diamonds denote the non-linear high-fidelity model (using the strains from the low-fidelity solution). The total elastic force acting on the beam is 6.652 mN using the low-fidelity model and 6.162 mN with the high-fidelity one, i.e. the non-linear behavior of the high-fidelity model leads to a 0.490 mN decrease in force.

Figure 8 shows the functional derivative of the total elastic force along r_3 with respect to the input constitutive law obtained numerically from equation (19). The derivative is positive for tensile axial strains, this indicates that stiffening the material in tension leads to an increase in restoring elastic force. On the other hand, the derivative is negative for compressive axial strains; an increase in the stress for negative strains, i.e. making the material softer in compression, leads to a decrease in the restoring force. We also see that the absolute value of the functional derivative increases with increasing strain (also in absolute terms) but is only non-zero for the strains present in the solution.

With the functional derivative at hand we can compute a correction to the QoI given the high-fidelity model using the functional UQ relationship in equation (5). We do this by numerical integration using the 50×50 grid on which the functional derivative was calculated; the correction is $-0.000\,490$ mN; this is identical to the actual value computed explicitly. As before this shows that when the QoI is a linear functional of the constitutive law the correction provided by functional UQ is exact.

We now explore the use of the functional derivative to rank in importance the evaluations of the high-fidelity model. Figure 9 shows the accumulated correction of restoring force as

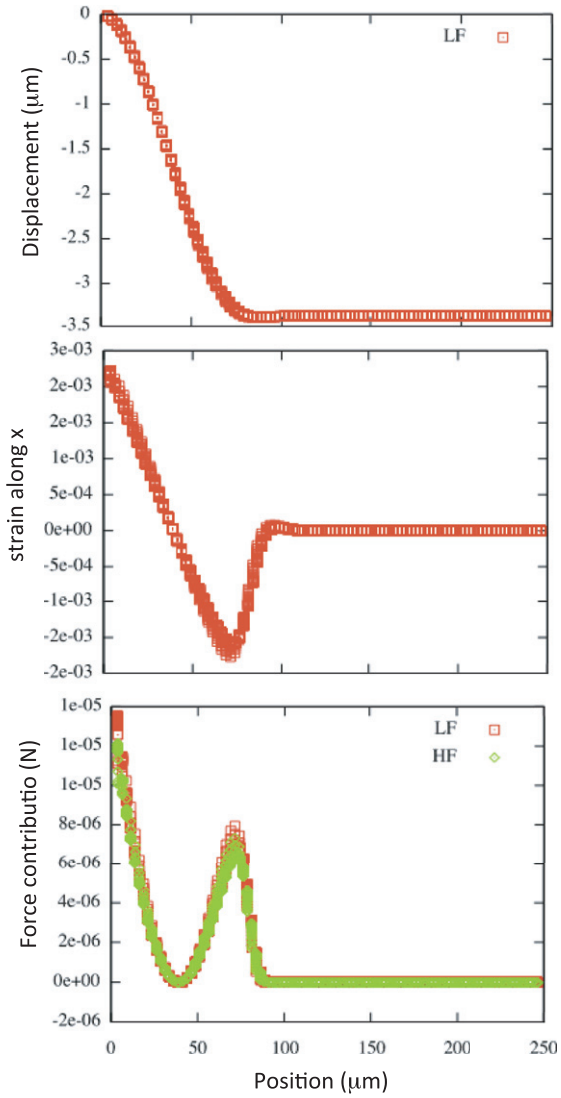

Figure 7. Results corresponding to the deformed beam. (*a*) Beam deflection along its length. (*b*) Longitudinal component of the strain as a function of position along length. (*c*) Contribution of force for each finite volume cell according to equation (17) using the low- and high-fidelity models.

a function of the number of high-fidelity model evaluations using the functional derivative expression (equation (5)). The high-fidelity model evaluations are ordered according to the absolute value of the functional sensitivity corresponding to the specific strains (i.e. we assume a uniform discrepancy). We see that an essentially exact correction is obtained with less than 250 high-fidelity model evaluations. The correction can also be evaluated explicitly from equation (16) and the individual contributions ranked in terms of the absolute value of the strain along r_1. Figure 9 compares the accumulated correction as a function of the number of high-fidelity model evaluations ordered in decreasing order of importance according to the functional derivative approach (equation (5)) and using an explicit evaluation using strain as ranking. The number of evaluations of the high-fidelity model is significantly reduced using the functional sensitivity approach while yielding an essentially exact correction.

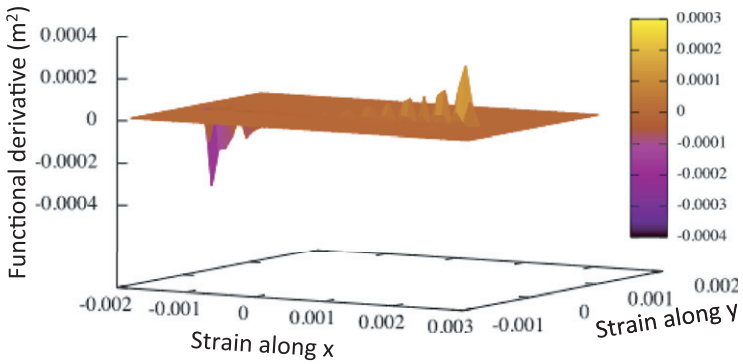

Figure 8. Functional derivative of the elastic force acting on the beam with respect to the stress–strain function calculated from equation (19).

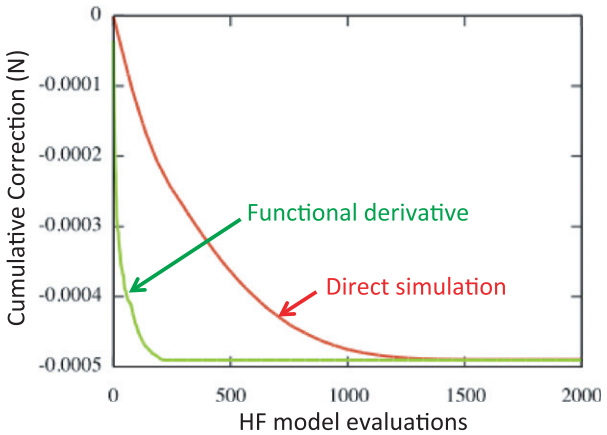

Figure 9. Correction to the low-fidelity model prediction of elastic force as a function of number of evaluations of the high-fidelity model. Green line shows results using the functional derivative approach equation (5) and ranking the high-fidelity evaluations based on their functional derivative and the red curve shows results obtained by a direct evaluation of the correction via equation (16) and ranking the evaluations based on the absolute value of the local strain along the beam axis.

We note that the number of high-fidelity model evaluations required for the correction based on functional UQ depends on the physics of the problem and the range of the constitutive law explored and is independent of the resolution and size of the physical simulation. We also note that computing the high-fidelity model correction explicitly requires knowing the complete state of the physical simulation (strain for all cells in our example); on the other hand, the exact correction can be obtained using the functional UQ approach with knowledge of the functional derivative alone. This makes the functional UQ approach attractive for large-scale simulations.

6. Discussion and conclusions

In summary, we extended the concept of sensitivity of a QoI with respect to input parameters to sensitivity with respect to input functions and showed that this functional sensitivity (the derivative of the QoI with respect to the entire constitutive law) can be used to estimate uncertainties with respect to the models used in the simulation, correct the predicted QoI

once a refined constitutive law becomes available and to rank potential on-demand physics-enhancement simulations designed to minimize the error in the prediction.

The sensitivity of the prediction of a deterministic code with respect to input parameters can be calculated via a variety of approaches with varying degrees of code intrusiveness, from generalized polynomial chaos modeling that requires solving a set of equations different from those in the deterministic model, to automatic code differentiation [21] that requires relatively minor changes to the original code and collocation that simply involves executing the deterministic code for various sets of input parameters. The proposed functional derivatives can be obtained in similar ways. For some problems, functional derivative expressions can be obtained analytically and implemented into simulation codes as was carried out in this paper. Alternatively, collocation approaches can be used by providing the constitutive laws in tabular form and varying the individual values. Automatic code differentiation should be explored as a possible efficient and non-intrusive approach to compute functional derivatives, during code execution. We foresee that computationally efficient ways of computing functional derivatives in complex physics and engineering codes together with the method presented here will provide invaluable information about the constitutive laws used in predictive simulations and will provide an important tool for the effective use of extreme-scale computing platforms.

The ability to predict materials properties or device performance with quantified uncertainties is expected to revolutionize design, optimization and certification cycles, significantly decreasing the cost and time involved in the deployment of new materials and devices. While experimental validation will always remain a critical step in this process, the continuing increase in computing power and advances in high-fidelity, first-principles, simulations with increased accuracy make quantification of predictions with respect to finer-scale models an important task. Examples of applications where high-fidelity models are becoming accurate enough to quantitative predictions include interatomic potentials for various fcc metals [22] to predict the mechanical response of high-purity poly-crystals [23] and *ab initio* calculations for an increasing range of electronic, structural and energetics predictions [24–28]. We foresee that macro- or device-scale predictions with rigorously quantified errors with respect to high-fidelity models that can be considered exact for the QoI will be an invaluable tool in predictive modeling and simulation and its use for design, optimization and certification. Furthermore, the ability to identify physics-enhancement simulations and their use to quantify and minimize uncertainties are likely to play a central role in the effective use of planned exascale computing systems that may enable pervasive physics enhancement in various applications.

Acknowledgments

This work was supported by the US Department of Energy's National Nuclear Security Administration under contract Grant No DE-FC52-08NA28617, Center for the Prediction of Reliability, Integrity and Survivability of Microsystems (PRISM). Fruitful discussions with M Koslowski are gratefully acknowledged.

Appendix: Surrogate models for functional discrepancy

In previous work, researchers have employed various types of surrogate models such as Gaussian process regression [17, 29]], radial basis functions [30], polynomial response surfaces [31, 32], Splines [33] and Polynomial Chaos Expansions [34, 35]. These models are based either on statistical or functional approximation theory and are known to be capable of approximating a wide class of function types [36].

Once a surrogate modeling technique is selected, the design of an approximate model then involves (1) selection of training points and (2) estimation of the internal parameters of the model. Since the mapping implied by the simulation is not known and is expensive to evaluate, the selection of the optimal training point distribution can neither be determined *a priori* nor be based on selection criteria based directly on the simulation which requires extensive evaluation. Consequently, sample selection is necessarily sequential and based on selection criteria defined on the intermediate estimates of the underlying function provided by the surrogate models and the functional sensitivity.

Typical approaches to training data selection belong to the variance reduction class of techniques that borrow from optimal experiment design methods [37]. Using the Bayesian approach, Mackay [38] and Tong [39] described entropy-based sample selection criteria for reduction of parameter uncertainty and model discrimination. These criteria are analogous to their counterparts in optimal experiment design. More recently, Guestrin *et al* [40] proposed a mutual information based criterion for reducing *a posteriori* prediction uncertainty in Gaussian process models and presented an approximate polynomial-time algorithm for the problem. Gramacy and Lee [41] employ Gaussian trees to represent non-stationary processes and employ prediction variance for the design of sample using the space-filling Latin hypercube designs [42].

6.1. Basics of Gaussian process regression

In Gaussian process regression (GPR), it is assumed that the underlying function values represent a particular realization of a Gaussian process, and the objective then is to identify the particular realization based on the training data [17]. The Gaussian process (GP) is a generalization of the multivariate Gaussian distribution and thus may be thought of as a collection (indexed by points in the domain) of multivariate Gaussian random variables. A GP is fully defined with the specification of the mean function, $m(z)$, and the covariance function $k(z, z')$. In general, these functions must be selected so as to reflect our assumptions about the underlying function, such as about its stationarity, periodicity, etc, [17, 38, 43]. As is common in the literature [17, 29], it is assumed below that the mean function, $m(\cdot) = 0$ and the covariance function is the squared exponential function:

$$\kappa\left(z_i, z_j, \theta\right) = \theta \exp\left[-\frac{1}{2}\sum_{d=1}^{D}\frac{\left(z_i^d - z_j^d\right)^2}{l_d}\right]. \tag{20}$$

Together, $\Theta = \{l, \theta_n, \sigma_n\}$ form the parameters of the covariance function and thus of the GP model. In order to be able to make predictions using the model, these parameters must be inferred from the given data. A common method employed is the maximization of the log marginal likelihood [17]. Of special interest are the parameters, $l = \{l_1, l_2, \ldots, l_D\}$ known as length-scale parameters, which correspond to the length of the variation in function values implied by $k(\cdot)$ in each dimension of Ω. A small value of l_d indicates significant variation in the function values in the dth dimension, a large value of l_d indicates that the variability in the function value is not impacted by changes in the dth dimension.

The GP predictive distribution is given by [17] $p(f_P|y_T, z_T, z_P, \Theta) \sim N(m, S)$ with

$$m = K_{PT}\left(K_{TT} + \sigma_n^2 I\right)^{-1} y_T \tag{21}$$

$$S = K_{PP} - K_{PT}\left(K_{TT} + \sigma_n^2 I\right)^{-1} K_{TP}, \tag{22}$$

where, $K_{TT} = [k(z_i, z_j)]_{i,j}$ is the $t \times t$ matrix of the covariances between the training points z_T, K_{PP} is the $p \times p$ matrix of the covariances between the prediction points z_P, and K_{PT}

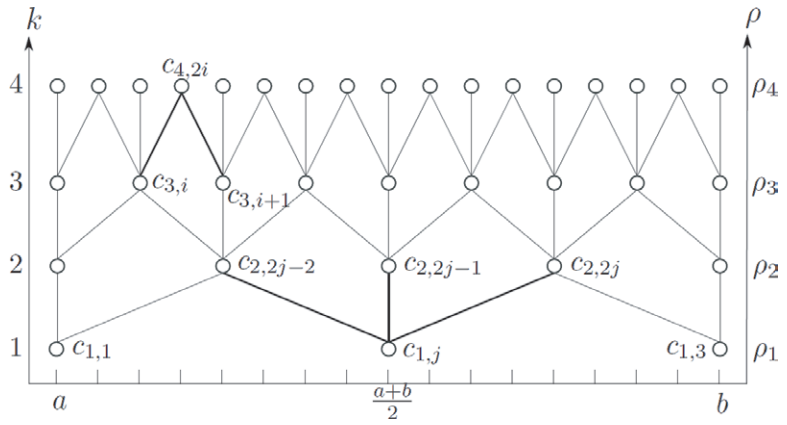

Figure 10. Analysis grid.

is the $p \times t$ matrix of covariances between z_P and z_T with K_{TP} as its transpose. The mean of the posterior distribution, m, is taken to be the predicted values of the underlying function at the z_P. This estimate is a function of (1) the measurement uncertainty, (2) the separation between the training points, (3) the measured value of the underlying function at the training points and (4) separation between the training points and the prediction points. By collecting all the terms that do not depend on the prediction points, z_P, equation (3) may be rewritten as follows

$$m = K_{PT} w_T. \tag{23}$$

If a computer code is used to evaluate f_T or y_T, then typically, there is no measurement noise and σ_n may be set to zero. Under such circumstances, the GPR model is interpolative, i.e. $m(x_T) = f_T$ and $S(z_T) = 0$. The covariance of the predicted values, S, represents the uncertainty in prediction, equation (23).

6.2. Application to discrepancy modeling

Among a set of locations at which the expensive high-fidelity model is evaluated, a subset of points (referred to as inducing inputs) is used to construct a GP model, and the discrepancy is evaluated at the remaining points. This procedure is formally represented as sparse Gaussian process (SGP) regression [44, 45]. The locations with high discrepancy are explored further with additional training points in that region. A simple option is a ternary tree in which each layer is a dyadic partition of the previous layer, as shown in figure 10 [30]. This adaptive exploration of the domain results in a hierarchical decomposition of the error, written as

$$\begin{array}{c|lcl} & e_1 & = & g, \\ k=1 & e_1 & = & \hat{e}_1 + e_2, \\ k=2 & e_2 & = & \hat{e}_2 + e_3, \\ \vdots & & \vdots & \\ k=M & e_M & = & \hat{e}_M + e_{M+1}. \end{array} \tag{24}$$

where, $k = \{1, 2, \ldots, M\}$ is the index to the M-level hierarchy. The first layer of the model approximates the discrepancy g with $\hat{e}_1$ and $e_2 = e_1 - \hat{e}_1$ is the corresponding approximation error. Similarly, in subsequent layers, $\hat{e}_k$ is the kth layer approximation to the error, e_k, in the

previous layer, and $e_{k+1} = e_k - \hat{e}_k$ is the corresponding approximation error of the current layer. See [18] for details of implementation.

References

[1] Dongarra J *et al* 2011 The international exascale software project roadmap *Int. J. High Perform. Comput. Appl.* **25** 3–60

[2] To A C *et al* 2008 Materials integrity in microsystems: a framework for a petascale predictive-science-based multiscale modeling and simulation system *Comput. Mech.* **42** 485–510

[3] Grice D *et al* 2009 Breaking the petaflops barrier *IBM J. Res. Dev.* **53** 1

[4] Barton N R, Bernier J V, Knap J, Sunwoo A J, Cerreta E K and Turner T J 2011 A call to arms for task parallelism in multi-scale materials modeling *Int. J. Numer. Methods Eng.* **86** 744–64

[5] Ceder G, Hautier G, Jain A and Ong S P 2011 Recharging lithium battery research with first-principles methods *MRS Bull.* **36** 185–91

[6] Strachan A and Goddard W A 2005 Large electrostrictive strain at gigahertz frequencies in a polymer nanoactuator: computational device design *Appl. Phys. Lett.* **86** 083103

[7] Lucas L J, Owhadi H and Ortiz M 2008 Rigorous verification, validation, uncertainty quantification and certification through concentration-of-measure inequalities *Comput. Method Appl. Mech.* **197** 4591–609

[8] Koslowski M and Strachan A 2011 Uncertainty propagation in a multiscale model of nanocrystalline plasticity *Reliab. Eng. Syst. Safety* **96** 1161–70

[9] Kouchmeshky B and Zabaras N 2010 Microstructure model reduction and uncertainty quantification in multiscale deformation processes *Comput. Mater. Sci.* **48** 213–27

[10] Jakeman J, Eldred M and Xiu D 2010 Numerical approach for quantification of epistemic uncertainty *J. Comput. Phys.* **229** 4648–63

[11] Ma X and Zabaras N 2011 A stochastic mixed finite element heterogeneous multiscale method for flow in porous media *J. Comput. Phys.* **230** 4696–722

[12] Ren X, Wu W and Xanthis L S 2011 A dynamically adaptive wavelet approach to stochastic computations based on polynomial chaos—capturing all scales of random modes on independent grids *J. Comput. Phys.* **230** 7332–46

[13] Hemez F 2003 Uncertainty quantification and the verification and validation of computational models *Damage Prognosis for Aerospace, Civil and Mechanical Systems* ed D Inman *et al* (London: Wiley)

[14] Frederiksen S L, Jacobsen K W, Brown K S and Sethna J P 2004 Bayesian ensemble approach to error estimation of interatomic potentials *Phys. Rev. Lett.* **93** 165501

[15] Wagner R, Moon R, Pratt J, Shaw G and Raman A 2011 Uncertainty quantification in nanomechanical measurements using the atomic force microscope *Nanotechnology* **2** 455703

[16] Greiner W and Reinhardt J 1996 *Field Quantization* (Berlin: Springer)

[17] Rasmussen C and Williams C 2006 *Gaussian Processes for Machine Learning* (Cambridge, MA: MIT Press)

[18] Hombal V and Mahadevan S 2011 Bias minimization in Gaussian process surrogate modeling for uncertainty quantification *Int. J. Uncertainty Quantification* **1** 321–49

[19] Peroulis D 2012 Capacitive MEMS Switches *Encyclopedia of Nanotechnology* 1st edn (Berlin: Springer)

[20] Das D, Mathur S R and Murthy J Y 2002 Finite-volume method for structural analysis of RF MEMS devices using the theory of plates *Numer. Heat Transfer* B **61** 1–21

[21] Mathur S R, Chigullapalli A and Murthy J Y 2010 A unified unintrusive discrete approach to sensitivity analysis and uncertainty propagation in fluid flow simulations *Proc. ASME IMECE (Vancouver, Nov. 2010)* vol. 11 pp 213–24

[22] Baskes M I, Srinivasan S G, Valone S M and Hoagland R G 2007 Multistate modified embedded atom method *Phys. Rev.* B **75** 16

[23] Derlet P, Gumbsch P, Hoagland R, Li J, Mcdowell D L, Swygenhoven H V and Wang J 2009 Atomistic simulations of dislocations in confined volumes *MRS Bull.* **34** 184

[24] Kolorenc J and Mitas L 2011 Applications of quantum Monte Carlo methods in condensed systems *Rep. Progr. Phys.* **74** 026502

[25] Bartlett R and Musiał M 2007 Coupled-cluster theory in quantum chemistry *Rev. Mod. Phys.* **79** 291–352

[26] Marzari N 2006 Realistic modeling of nanostructures using density functional theory *MRS Bull.* **31** 681

[27] Anderson N L, Vedula R P, Schultz P A, Ginhoven R M V and Strachan A 2011 First-principles investigation of low energy E' center precursors in amorphous silica *Phys. Rev. Lett.* **106** 206402

[28] Schultz P A 2006 Theory of defect levels and the 'band gap problem' in silicon *Phys. Rev. Lett.* **96** 4

[29] Sacks J, Welch W, Mitchell T and Wynn H 1989 Design and analysis of computer experiments *Stat. Sci.* **4** 409–35

[30] Powell M 1987 Radial basis functions for multivariable interpolation: a review *Algorithms for Approximation* (Oxford: Clarendon) pp 143–67
[31] Ma X and Zabaras N 2009 An adaptive hierarchical sparse grid collocation algorithm for the solution of stochastic differential equations *J. Comput. Phys.* **228** 3084–113
[32] Simpson T, Poplinski J, Koch P and Allen J 2001 Metamodels for computer-based engineering design: survey and recommendations *Eng. Comput.* **17** 129–50
[33] Wahba G 1990 Spline models for observational data *CBMS-NSF Regional Conference Series in Applied Mathematics* based on a series of 10 lectures at Ohio State University at Columbus, 23–27 March 1987 (Philadelphia, PA: SIAM)
[34] Eldred M, Webster C and Constantine P 2008 Evaluation of non-intrusive approaches for wieneraskey generalized polynomial chaos *Proc. 10th AIAA Non-Deterministic Approaches Conf. (Schaumburg, IL, 2008)* number AIAA-2008-1892
[35] Ghanem R and Spanos P 2003 *Stochastic Finite Elements: a Spectral Approach* (New York: Dover)
[36] Kennedy M and O'Hagan A 2001 Bayesian calibration of computer models *J. R. Stat. Soc.* B **63** 425–64
[37] Cohn D, Ghahramani Z and Jordan M 1996 Active learning with statistical models *J. Artif. Intell. Res.* **4** 129–45
[38] MacKay D 1992 Information-based objective functions for active data selection *Neural Comput.* **4** 590–604
[39] Tong S 2001 Active learning: theory and applications *PhD Thesis* Stanford University
[40] Guestrin C, Krause A and Singh A 2005 Near-optimal sensor placements in Gaussian processes *Machine Learning-International Workshop The Conf. (Bonn, Germany)* vol 22 p 265
[41] Gramacy R, Lee H and Macready W 2004 Parameter space exploration with Gaussian process trees *Proc. 21st Int. Conf. on Machine Learning (Banff, Canada)* (New York, NY: ACM Press)
[42] Box G, Hunter W and Hunter J 1978 Statistics for experimenters: an introductory to design data analysis and model building (*Wiley Series in Probability and Mathematical Statistics*) (London: Wiley)
[43] Paciorek C 2003 Nonstationary Gaussian processes for regression and spatial modelling *PhD Thesis* Carnegie Mellon University
[44] Smola A and Bartlett P 2001 Sparse greedy Gaussian process regression *Advances in Neural Information Processing Systems* vol 13 (Denver, CO: Neutral Information Processing Systems Foundation)
[45] Snelson E and Ghahramani Z 2006 Sparse Gaussian processes using pseudo-inputs *Advances in Neural Information Processing Systems* vol 18 (Cambridge, MA: MIT Press), p 1257